PERGAMON

International Journal of Heat and Mass Transfer 45 (2002) 4435–4450

International Journal of HEAT and MASS TRANSFER

www.elsevier.com/locate/ijhmt

Comparison of CHF measurements in horizontal and vertical tubes cooled with R-134a

I.L. Pioro [a,*], D.C. Groeneveld [a,b], L.K.H. Leung [a], S.S. Doerffer [c], S.C. Cheng [b], Yu.V. Antoshko [b], Y. Guo [b], A. Vasić [b]

[a] *Chalk River Laboratories, AECL, Chalk River, Ont., Canada K0J 1J0*
[b] *Department of Mechanical Engineering, University of Ottawa, Ottawa, Ont., Canada K1N 6N5*
[c] *AECL, Sheridan Park Mississauga, Ont., Canada L5K 1B2*

Received 14 January 2002; received in revised form 12 April 2002

Abstract

An experimental study of the critical heat flux (CHF) in horizontal and vertical tubes cooled with R-134a has been completed. The investigated ranges of flow parameters in R-134a were outlet pressures of 1.31, 1.67 and 2.03 MPa (8, 10 and 12 MPa in water-equivalent values), mass flux from 500 to 3000 $kg\,m^{-2}\,s^{-1}$ (700–4300 $kg\,m^{-2}\,s^{-1}$ in water-equivalent values), and critical quality from −0.1 to +0.9. The wide range of qualities was achieved using tubes of different heated lengths and two-phase flow at the test-section inlet.

The R-134a CHF data obtained in the vertical orientation agreed with the R-134a-equivalent CHF values from the water-based CHF look-up table. The effect of orientation on CHF was found to depend on mass flux, quality and pressure, as well as the limiting critical quality. This effect is strong at low mass fluxes, but disappears at high mass fluxes. At qualities higher than the limiting critical qualities, the CHF in horizontal flow can be greater than the corresponding value in vertical flow at the same critical quality conditions. A maximum reduction in CHF due to flow stratification was observed at qualities between the limiting critical qualities for horizontal and vertical flows.

The orientation effect on CHF appears to be much stronger for R-134a than for water flow at the same critical quality, equivalent mass flux (based on vertical flow fluid-to-fluid modeling relationships) and density ratio. This behavior is primarily due to the larger density difference between liquid and vapor and the lower vapor velocity in R-134a.

Keywords: Critical heat flux; Flow boiling; Horizontal; Vertical; Tube; Refrigerant

1. Introduction

The objective of this study is to investigate the effect of orientation on the critical heat flux (CHF) over a wide range of qualities, including the limiting critical quality region. Knowledge of the CHF and dryout phenomenon in horizontal channels is important because of the many industrial applications: steam generators, horizontal tube evaporators, nuclear reactors, horizontal forced-circulation waste heat boilers, refrigerators, air-conditioning systems, and heat pumps. However, the literature on the orientation effect is quite limited.

Some heat-transfer laboratories use refrigerants to model the CHF in water, in both vertical and horizontal channels [1,2]. This is acceptable for horizontal flow at high mass flux conditions, where buoyancy forces are not important. However, for low-flow horizontal channels, no satisfactory CHF fluid-to-fluid modeling methodology is yet available. To ensure that the reference CHF data obtained in R-134a in vertical tubes are

* Corresponding author. Tel.: +1-613-584-8811x4805; fax: +1-613-584-1349.
E-mail address: pioroi@aecl.ca (I.L. Pioro).

0017-9310/02/$ - see front matter
PII: S0017-9310(02)00149-7

Nomenclature

D	inside diameter (m)
$G = \rho u$	mass flux ($kg\,m^{-2}\,s^{-1}$)
g	acceleration due to gravity ($m\,s^{-2}$)
H	enthalpy ($kJ\,kg^{-1}$)
H_{fg}	latent heat of vaporization ($kJ\,kg^{-1}$)
L	heated length (m)
p	pressure (MPa)
q	heat flux ($kW\,m^{-2}$)
u	velocity ($m\,s^{-1}$)
x_a	actual vapor quality
x	vapor quality (thermodynamic)
x_{cr}^{lim}	limiting critical quality (thermodynamic)
Greek symbols	
α	void fraction
Δ	difference
δ	thickness (mm)
μ	dynamic viscosity ($Pa\,s^{-1}$)
ρ	density ($kg\,m^{-3}$)
σ	surface tension ($N\,m^{-1}$)
Subscripts	
cal	calculated
cr	critical
f	saturated liquid
g	saturated vapor
hor	horizontal
in	inlet
l	subcooled liquid
lim	limiting
max	maximum
min	minimum
R	R-134a
vert	vertical
W	Water
w	wall

reliable, these data were compared with corresponding CHF data obtained in water-cooled tubes. Such comparison requires that the water data first be converted into refrigerant-equivalent values using the following commonly accepted CHF fluid-to-fluid modeling relationships [3,4]:

- Geometric similarity:

$$L_R = L_W, \quad D_R = D_W \tag{1}$$

- Hydrodynamic similarity

$$\left[\frac{G}{\left(\frac{\rho_f \sigma}{D}\right)^{0.5}}\right]_R = \left[\frac{G}{\left(\frac{\rho_f \sigma}{D}\right)^{0.5}}\right]_W \tag{2}$$

$$\left(\frac{\rho_f}{\rho_g}\right)_R = \left(\frac{\rho_f}{\rho_g}\right)_W \tag{3}$$

- Thermodynamic similarity

$$x_{cr\,R} = x_{cr\,W} \tag{4}$$

If these similarities are satisfied, then the dimensionless CHF, which is expressed as

$$\left[\frac{q_{cr}}{GH_{fg}}\right]_R = \left[\frac{q_{cr}}{GH_{fg}}\right]_W \tag{5}$$

will also be the same for both fluids (note that subscript R refers to refrigerant and subscript W to water).

The CHF look-up table [5] was used in the comparison, as it represents a normalized CHF database for vertical upward flow of water in 8-mm tubes. The table was converted into the R-134a-equivalent conditions using Eqs. (1)–(5). A simple correction was applied for tubes whose diameter was different from the reference 8 mm:

$$\frac{CHF_D}{CHF_{D=8\,mm}} = \left(\frac{D}{8}\right)^n \tag{6}$$

where D is the inside diameter of a circular tube in mm, and the commonly accepted value of the exponent n is -0.5 [5]. The combination of the look-up table and fluid-to-fluid modeling, as described above, permits comparisons of CHF data sets for different fluids and different diameters.

2. Literature review

2.1. Experiments

Becker [6] identified the various flow regimes during flow boiling along the length of a horizontal tube: single-phase flow, bubbly flow, plug flow, slug flow, wavy flow, and annular flow. He concluded that, at the beginning of wavy flow, an upstream dryout at the top of the tube can occur, in addition to that occurring at the tube end (downstream dryout).

Robertson [7] investigated the CHF in horizontal water-cooled tubes. He found that the limiting critical quality region can occur in both horizontal and vertical tubes, and that the CHF drop in that region in vertical tubes can be much more severe than in horizontal tubes. The limiting critical quality region in horizontal tubes appeared at lower qualities, compared to vertical tubes.

Merilo [8] conducted experiments in R-12 and water in horizontal tubes. He observed upstream dryout in horizontal tubes over a wide range of mass fluxes. Based on the experimental data, it was stated that scaling laws for CHF in vertical tubes do not apply to horizontal tubes, except at high mass fluxes, where the difference in CHF values between vertical and horizontal tubes disappears. In a later paper, Merilo [9] proposed new criteria for the fluid-to-fluid modeling of CHF in horizontal tubes. However, no single set of fluid-to-fluid modeling criteria can work well within the full range of critical qualities and mass fluxes because of the presence of different CHF mechanisms, especially on both sides of the limiting critical quality regions in vertical and horizontal tubes.

Merilo and Ahmad [10] studied the orientation and diameter effects on CHF in tubes (ID of 5.3 and 12.6 mm) using R-12 as coolant. The investigated range covered two pressures (1.05 and 1.52 MPa), mass fluxes from 1600 to 8100 $\mathrm{kg\,m^{-2}\,s^{-1}}$, and heated lengths from 1.03 to 3.05 m. Merilo and Ahmad [10] found that, at low mass flux values, the CHF was lower for horizontal flow than for vertical flow. With increasing mass flux, the vertical and horizontal CHF results converged. At mass fluxes of 4000 $\mathrm{kg\,m^{-2}\,s^{-1}}$ and above, the CHF values were essentially identical. The observed diameter effect on CHF depended on the analysis approach. That is, for the constant inlet conditions approach, the diameter effect in horizontal flow was expressed as $\mathrm{CHF} \sim (D_{12.6}/D_{5.3})^{0.36}$ and in vertical flow, $\mathrm{CHF} \sim (D_{12.6}/D_{5.3})^{0.4}$ at $p = 1.05$ MPa, $G = 2720$ $\mathrm{kg\,m^{-2}\,s^{-1}}$, $x_{\mathrm{in}} = -0.1$, and $L = 2.44$ m. For the constant critical quality approach at $p = 1.05$ MPa, the diameter effect in horizontal flow was expressed as $\mathrm{CHF} \sim (D_{12.6}/D_{5.3})^{-0.63}$ at $x_{\mathrm{cr}} = 0.3$, and in vertical flow, $\mathrm{CHF} \sim (D_{12.6}/D_{5.3})^{-0.64}$ at $x_{\mathrm{cr}} = 0.4$. A vertical drop in CHF was present in their plots of CHF versus critical quality. However, this CHF drop was not identified as a limiting critical quality phenomenon.

Köhler and Hein [11] performed a detailed study on flow boiling in vertical and horizontal tubes with water. From their measured CHF locations and wall-temperature distribution (axially and around the tube perimeter), they postulated the existence of various two-phase flow regimes. Fig. 1 shows the variation in CHF and wall temperature along the top and bottom of a horizontal tube, for a mass flux of 500 $\mathrm{kg\,m^{-2}\,s^{-1}}$ and a pressure of 10 MPa. The drypatch locations are also shown schematically. Köhler and Hein's findings are in agreement with those of Becker [6].

2.2. Predictions of the orientation effect on CHF

Taitel and Dukler [12] developed a model for flow regime transitions in horizontal and near-horizontal two-phase gas–liquid flow. A generalized flow regime map that is valid for a wide range of fluids and flow conditions was proposed.

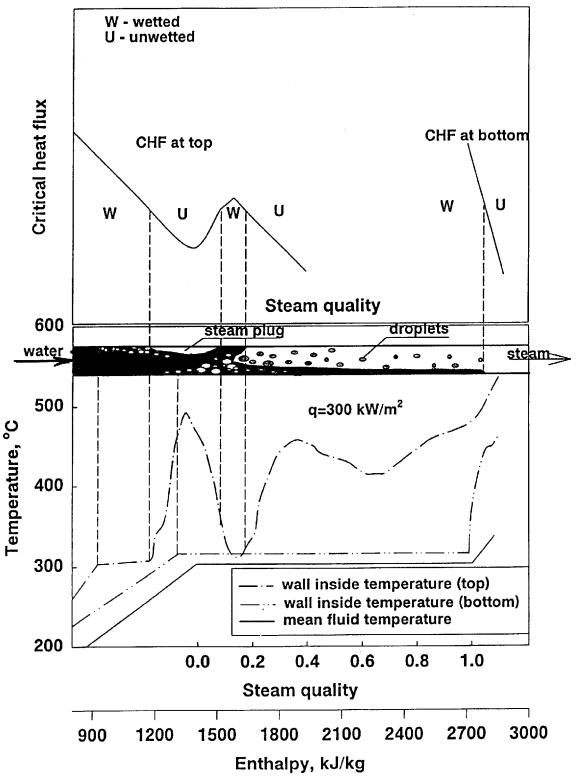

Fig. 1. Effect of gravity on heat transfer and CHF in horizontal tube [11]: water, $p = 10$ MPa, $G = 500$ $\mathrm{kg\,m^{-2}\,s^{-1}}$, $D = 24.3$ mm.

Merilo [9] developed the following non-dimensional equation for predicting the CHF in horizontal flow:

$$\frac{q_{\mathrm{cr}}}{GH_{\mathrm{fg}}} = 575Re^{-0.340}(Z^3Bo)^{0.358}\left(\frac{\mu_{\mathrm{f}}}{\mu_{\mathrm{g}}}\right)^{-2.18}\left(\frac{L}{D}\right)^{-0.511} \times \left(\frac{\rho_{\mathrm{f}}}{\rho_{\mathrm{g}}} - 1\right)^{1.27}(1 - x_{\mathrm{in}})^{1.64} \tag{7}$$

where $q_{\mathrm{cr}}/GH_{\mathrm{fg}}$ is the Boiling number, $Re = GD/\mu_{\mathrm{f}}$ is the Reynolds number, $Z = \mu_{\mathrm{f}}/\sqrt{\sigma D\rho_{\mathrm{f}}}$ is the Ohnesorge number, and $Bo = (\rho_{\mathrm{f}} - \rho_{\mathrm{g}})gD^2/\sigma$ is the Bond number. Eq. (7) correlates 462 R-12 and 143 water data points, with an rms error of about 9%. However, the analysis of the present R-134a data showed poor agreement of the data with the above prediction method in some flow conditions.

Groeneveld et al. [13] slightly modified the Taitel–Dukler flow regime map, and postulated that the CHF varied from a value that was equal to the vertical tube CHF at the homogeneous annular flow regime, to a value of zero at the stratified flow regime boundary, where the waves were assumed to be unable to wet the

top part of the tube. Groeneveld et al. [13] proposed the use of a correction factor to relate the CHF in horizontal tubes to the corresponding value for vertical flow, for the same value of pressure, mass flux, and x_{cr}:

$$q_{cr\,hor} = Kq_{cr\,vert} \tag{8}$$

where $q_{cr\,vert}$ is the reference CHF value for vertical flow from the water-based look-up table [5]. Thus, a CHF correction factor K to the vertical tube case was proposed, which varied linearly from 0.0 to 1.0, based on the dimensionless groups that were used for predicting the flow regime boundaries. Later on, Wong et al. [14] proposed an analytically-based expression for K:

$$K = 1 - \exp\left[-\left(\frac{\vartheta}{C_1}\right)^{0.5}\right] \tag{9}$$

$$\vartheta = C_2 Re^{-0.2}\left(\frac{1-x_a}{1-\alpha}\right)^2 \frac{G^2}{gD\rho_f(\rho_f-\rho_g)\alpha^{0.5}} \tag{10}$$

where C_1 and C_2 are constants ($C_1 = 3$ [14] and $C_2 = 0.046$ [15]), $Re = (GD/\mu_f)(1-x_a)$ is the Reynolds number, x_a is the actual vapor quality, and α is the void fraction. This method of calculating CHF in horizontal tubes based on Eqs. (8)–(10) requires different correlations and iteration techniques, when there is non-equilibrium between the phases, i.e., for low qualities and subcooled conditions. Wong [16] suggested using the Saha and Zuber correlation [17] to evaluate x_a. The approach of Groeneveld and Wong was recommended by Tong and Tang [18].

The ESDU [19] proposed a method that was based on a correlation for the ratio CHF_{vert}/CHF_{hor}. This ratio depends primarily on a mass flux ratio, i.e., the ratio of the actual mass flux to the minimum mass flux that is necessary to avoid flow stratification.

Kefer et al. [20] studied the orientation effect on CHF in inclined tubes (inclination angles 0°, 15°, 30° and 90°, and tube IDs of 12.5 and 24.3 mm) using water as the coolant. The investigated range covered pressures from 2.5 to 20 MPa, mass fluxes from 300 to 2500 $kg\,m^{-2}\,s^{-1}$, and a heated length of 7 m. A modified Froude number was introduced to quantify the effect of orientation, and is defined as

$$Fr = \frac{x_{cr}G}{\left[g\cos\phi\, D\rho_g(\rho_f-\rho_g)\right]^{0.5}} \tag{11}$$

where ϕ is the channel inclination angle ($\phi = 0°$ corresponds to a horizontal tube). Kefer et al. [20] observed that the stratification effects are pronounced for Froude numbers less than 7. At $Fr \geqslant 10$, the orientation effect has no impact on dryout.

Celata and Mariani [21] proposed setting a limit for the effect of tube orientation on CHF in flow boiling, based on a value of their version of a modified Froude number:

$$Fr = \frac{G\cos\phi}{\rho_f\left[gD\left(\frac{\rho_f-\rho_g}{\rho_f}\right)\right]^{0.5}} \tag{12}$$

They found that the effect of orientation disappears at $Fr > 5$–7. However, the experiments with water flow boiling in horizontal and vertical tubes by Celata et al. [22] showed that the orientation effect disappears at higher values of the Froude number ($Fr > 20$).

2.3. Limiting critical quality in horizontal flow

The limiting critical quality phenomenon refers to a sharp change in the slope of the CHF versus x_{cr} trend at the so-called "limiting critical quality", or x_{cr}^{lim} value, which depends on flow conditions and tube diameter. The rapid change in the CHF versus x_{cr} slope is caused by a change in the CHF mechanism in the annular flow regime, from the so-called *entrainment-controlled dryout* to *deposition-controlled dryout*. Entrainment-controlled dryout is typical for $x_{cr} < x_{cr}^{lim}$, where the liquid film is fairly thick, and is depleted by a combination of entrainment and evaporation. During deposition-controlled dryout, the liquid film is too thin to permit significant entrainment, and film dryout can only be prevented by significant droplet deposition [23].

The evidence for the existence of this phenomenon in water CHF tests for vertical upflow was reviewed by Kitto [24], and has been confirmed recently by Pioro et al. [3,25–29]. This limiting critical quality phenomenon can result in a significant CHF reduction (under some flow conditions, CHF can be reduced by up to 15 times in vertical tubes [3]).

The limiting critical quality phenomenon has also been observed in horizontal flow. Kutepov et al. [30] summarized findings in Russian literature regarding differences in the limiting critical quality values in horizontal and vertical flows.

Merilo and Ahmad [10] measured the CHF in a horizontal tube in R-12, at a mass flux of 2700 $kg\,m^{-2}\,s^{-1}$. They noticed very steep portions of the CHF versus critical quality curve, which are typical of the limiting critical quality phenomenon.

Köhler and Hein [11] conducted CHF experiments with water in horizontal tubes, and also found that at some flow conditions, the CHF drops rapidly at an almost constant critical quality value.

More details about the limiting critical quality in horizontal and vertical tubes cooled with water and R-134a can be found in Pioro et al. [31].

2.4. Conjugated effect

An additional effect that may mitigate the temperature excursion at CHF in horizontal tubes is the conjugated effect (due to circumferential heat conduction within the

tube wall) [11,32–34]. According to Pioro et al. [33,34], variations in tube wall thickness from 0.5 to 3 mm, and/or variations in the value of the thermal conductivity coefficient from 15 (stainless steel) to 400 $W\,m^{-1}\,K^{-1}$ (copper) can increase the CHF values up to two times.

3. Experiments

3.1. General

The experimental study was performed in the University of Ottawa's multi-fluid loop, using R-134a as a coolant. The main components of the loop are the test section (which can be oriented horizontally or vertically), the condenser, the pressurizer, the preheater, the heat exchanger, two pumps (connected in series), power supplies for the test section (DC, maximum 40 V × 300 A) and for the preheater (DC, maximum 40 V × 150 A), and related instrumentation (flow meter, thermocouples, data acquisition system, voltmeter, ammeter, pressure transducer with sensor, etc.). Further details may be found in [3].

3.2. Test section

The same test section was used for the vertical and horizontal channel tests: an Inconel 601 tube, with a 6.92-mm ID and a maximum heated length of 2 m. The tube was electrically heated by direct current. The heated length was varied to provide a maximum variation in critical quality. To detect dryout, thirty pairs (located at the top and bottom of the test section) of fast-response K-type thermocouples with self-adhesive backings were used.

3.3. Test procedure

Before each series of CHF experiments, a heat-balance test was performed to check whether all instrumentation systems were working correctly. As well, CHF points were periodically measured (at fixed conditions) to assure the repeatability of the data. A comparison of the repeat CHF points over a period of several years did not show any significant differences (about 1%) [3].

Just prior to CHF occurrence, all test conditions were stabilized, and the power to the test section was raised in small steps. *CHF was defined as the first detected occurrence of a wall temperature excursion at the downstream end. All CHF data points presented here were obtained when the dryout location was just upstream of the power terminal at the test section exit.* For the horizontal test section, CHF always occurred first at the top of the test section; for several test series, subsequent CHF occurrences at the bottom of the test section were also obtained. At CHF, all values of the parameters were recorded. In preparation for the next run, the power to the test section was decreased, and the coolant temperature at the test section was changed to the next matrix value (the usual inlet temperature increment was about 2–3 °C). To extend the critical quality range to higher values, two-phase flow at the test section inlet was used for the maximum heated length of 2 m. Two-phase flow was generated in the electrically heated preheater by resistance heating. The outlet quality from the preheater was calculated from a heat balance, and this value was used as the inlet quality to the test section. To check that two-phase flow at the test section inlet does not introduce additional uncertainties to the CHF, additional measurements were obtained with shorter heated lengths and a two-phase inlet. This resulted in an overlap on a CHF versus x_{cr} plot of single-phase and two-phase inlet data (see also Section 4.2). No significant effect of the two-phase inlet on CHF was noted.

The test conditions are listed in Table 1. The inlet temperature ranged from the lowest possible value to the saturation temperature. The minimum inlet temperature depended on the cooling water temperature, and varied from 3 °C in winter to 22 °C in summer. The equivalent water-based conditions are also shown in Table 1.

3.4. Experimental errors

Heat balance tests showed that the heat loss ranged from 0% to 2% (in absolute values, not more than 20 W for the test section, and 50 W for the preheater) of the total power input. CHF measurement errors were less than 3.5% (5.5% for the experiments with two-phase flow at the inlet). Errors for measuring mass flux and pressure were less than 0.3% and 1%, respectively. The temperatures were measured with an accuracy better than ±0.5 °C.

4. Test results

4.1. General

The tests results are presented graphically in three ways:

Table 1
Test matrix conditions in R-134a and their water-equivalent values

p_R (MPa)	p_W (MPa)	G_W, $kg\,m^{-2}\,s^{-1}$			
1.31	8	–	1423	2846	4269
1.67	10	707	1415	2830	4245
2.03	12	–	1398	2796	–
		G_R, $kg\,m^{-2}\,s^{-1}$			
		500	1000	2000	3000

- As CHF versus critical quality. This permits the combination of all data obtained for a given pressure and mass flux, irrespective of heated length (which varied from 0.45 to 2 m) or two-phase flow inlet. The R-134a-equivalent data from the water-based look-up table for vertical tubes [5] were added to the plots. The critical quality was calculated as follows:

$$x_{cr} = x_{in} + \frac{4q_{cr}L}{GDH_{fg}}, \tag{13}$$

where $x_{in} = (H_{l\,in} - H_f)/H_{fg}$.

- As CHF versus inlet quality, for all heated lengths that were tested.
- As CHF versus inlet quality, for one normalized heated length (1.98 m). This permitted the combination of all heated lengths and single- and two-phase flow inlet data. The latter comparison provided an extra check on the consistency of the data, because the CHF versus x_{in} plots generally show a linear trend for $x_{in} < 0$. The conversion to the equivalent heated length of 1.98 m uses an adjustment that adds an extra heated length (ΔL) to the shorter tubes and lowers the inlet enthalpy by $\Delta H'_{in}$, such that the heat balance across the added heated ΔL is satisfied. The inlet quality for the normalized heated length is calculated according to

$$x_{in}|_{L=1.98\,m} = x_{in}|_L - \frac{4q_{cr}(1.98 - L)}{GDH_{fg}} \tag{14}$$

where $x_{in}|_L = (H_{l\,in} - H_f)/H_{fg}$.

Also, the data from the look-up table were converted into inlet quality conditions as follows: (i) through scaling laws (Eqs. (1)–(5)), the CHF data were converted from water to equivalent R-134a conditions; (ii) according to Eq. (6), the correction for D was applied; and (iii) through the following equation, the value of inlet quality was determined based on the same normalized heated length ($L = 1.98$ m) as the rest of the experimental data:

$$x_{in}|_{L=1.98\,m} = x_{cr} - \frac{4q_{cr}1.98}{GDH_{fg}}, \tag{15}$$

4.2. CHF versus critical quality

Figs. 2a, 3a,d, 4a, 5a,c, 6a,c, 7a and c show the CHF as a function of x_{cr} for all test conditions. Each figure shows the CHF data obtained in vertical and horizontal tubes and the CHF R-134a-equivalent predictions from the CHF look-up table [5], adjusted to a 6.92-mm-ID vertical tube. Where obvious, the limiting critical quality for each orientation is also shown in the graphs. The graphs generally confirm the expected behavior, i.e., (i) for high mass fluxes, the CHF for vertical and horizontal channels is the same, and (ii) for lower mass fluxes, the CHF in horizontal channels can be significantly lower than in vertical channels. A unique feature of this experiment was the wide range of critical qualities. This range permitted three separate regions to be distinguished over the mass flux range of 500–2000 kg m^{-2} s^{-1}: Region I for $x_{cr} < x^{lim}_{cr\,hor}$, Region II for $x^{lim}_{cr\,hor} < x_{cr} < x^{lim}_{cr\,vert}$, and Region III for $x_{cr} > x^{lim}_{cr\,vert}$ (the regions are added to Figs. 2a and 3a). Each region appeared to have

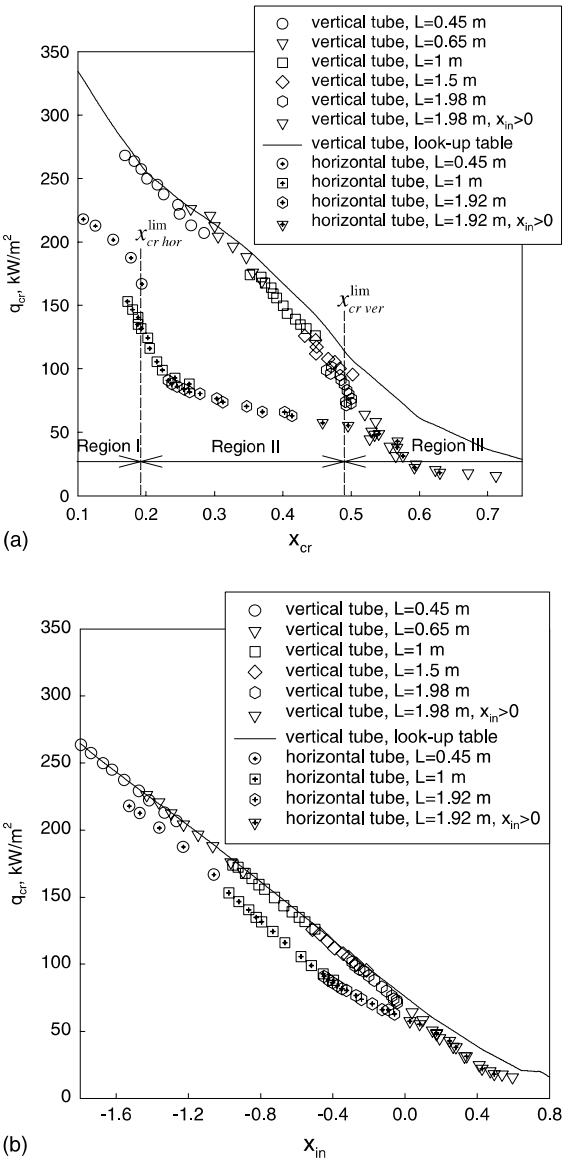

Fig. 2. Effect of quality on CHF in vertical and horizontal tubes ($D = 6.92$ mm): R-134a, $p = 1.31$ MPa, $G = 1000$ kg m^{-2} s^{-1}. (a) Effect of x_{cr}, (b) effect of x_{in}, data for tubes $L = 0.45$, 0.65, 1, 1.5 and 1.92 m converted to $L = 1.98$ m; look-up table, $L = 1.98$ m.

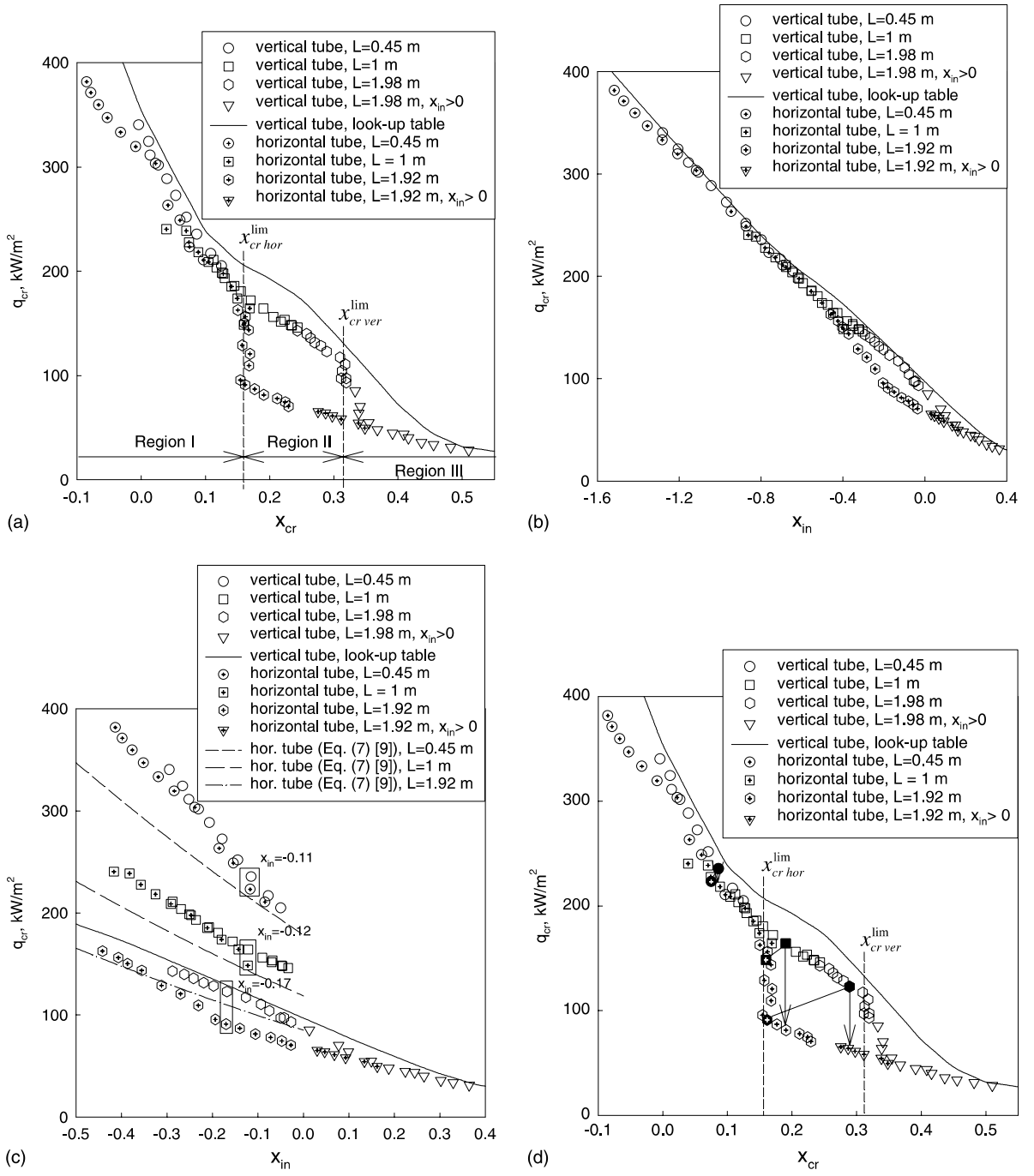

Fig. 3. Effect of quality on CHF in vertical and horizontal tubes ($D = 6.92$ mm): R-134a, $p = 1.31$ MPa, $G = 2000$ kg m^{-2} s^{-1}. (a) Effect of x_{cr}, (b) effect of x_{in}, data for tubes $L = 0.45$, 1 and 1.92 m converted to $L = 1.98$ m; look-up table, $L = 1.98$ m, (c) effect of x_{in}, pairs of symbols in rectangulars for details see (d), (d) effect of x_{cr}, pairs of closed symbols connected with solid lines have same values of inlet quality and heated length (see (c)), arrows show comparison for x_{cr} = constant.

a different CHF_{hor}/CHF_{vert} ratio, and the following general observations were made:

- The largest decrease in CHF due to the orientation effect appears to be in Region II, while in Region I,

the decrease in CHF is less pronounced or disappears altogether, as shown in Figs. 3a, 6a and 7c at $G = 2000\ \mathrm{kg\,m^{-2}\,s^{-1}}$.

- In Region III, the orientation effect on CHF disappears (Figs. 2a, 3a and 7c), or the CHF for horizontal flow becomes greater than that for vertical flow (Figs. 5a,c, 6a and 7a).
- For all tested pressures and at a mass flux of 3000 $\mathrm{kg\,m^{-2}\,s^{-1}}$, there is practically no difference in the CHF for both orientations (an exception can be seen at $p = 1.31$ MPa, where there is some difference beyond $x_{\mathrm{cr\,hor}}^{\mathrm{lim}}$, see Fig. 4a).
- The limiting critical quality phenomenon is fairly pronounced for both flow orientations at lower mass flux values ($G \leqslant 2000\ \mathrm{kg\,m^{-2}\,s^{-1}}$, see Figs. 2a, 3a, 5a, 6a and 7a). The differences between the limiting critical quality values for both orientations, $x_{\mathrm{cr\,vert}}^{\mathrm{lim}}$ and $x_{\mathrm{cr\,hor}}^{\mathrm{lim}}$, become smaller with increasing mass flux and pressure. This phenomenon is less pronounced or disappears altogether at mass fluxes of 3000 $\mathrm{kg\,m^{-2}\,s^{-1}}$ (Figs. 4a, 6c and 7c). At some flow conditions, the limiting critical quality is less pronounced for a horizontal tube than for a vertical tube (see Figs. 5c and 7a).

Figs. 5c, 6a and c distinguish between the CHF occurrence on the top of the horizontal tube, and the subsequent CHF on the bottom. Note that the bottom CHF values are always higher than the top CHF values (Figs. 5c–6d). This is true even for high mass fluxes ($G = 3000\ \mathrm{kg\,m^{-2}\,s^{-1}}$, see Fig. 6c). This suggests that the liquid film distribution in a horizontal tube is still not uniform at $G = 3000\ \mathrm{kg\,m^{-2}\,s^{-1}}$, with a thicker liquid film on the bottom.

At a high mass flux of 3000 $\mathrm{kg\,m^{-2}\,s^{-1}}$ and lower pressures of 1.31 and 1.67 MPa (Figs. 4a and 6c), and at a mass flux of 2000 $\mathrm{kg\,m^{-2}\,s^{-1}}$ and a high pressure of 2.03 MPa (Fig. 7c), there is good agreement between the horizontal (and also vertical) CHF data and the CHF look-up table predictions [5].

The CHF results obtained with two-phase flow at the test section inlet (Figs. 2a, 3a,d, 4a, 5a,c, 6a,c, 7a and c) show acceptable agreement with single-phase inlet data obtained at the same local conditions.

4.3. CHF versus inlet quality

Figs. 2b, 3b, 4b, 5b,d, 6b,d, 7b and d, present the CHF results as a function of adjusted inlet quality for the normalized heated length of 1.98 m. Only Fig. 3c shows the CHF data for each individual heated length. As found previously, the differences in CHF obtained in horizontal and vertical tubes, and the differences between the CHF results and the predictions based on constant x_{in} are much smaller than in the previous comparisons (Figs. 2a, 3a,d, 4a, 5a,c, 6a,c, 7a and c) for constant x_{cr}. In general, a linear relationship exists between CHF and x_{in} within a wide range of inlet qualities. Only at positive inlet qualities we can note a slight deviation from the linear trend. This change in slope was expected; the CHF would have become negative at x_{in} between 0.4 and 0.6, if the linearity had continued.

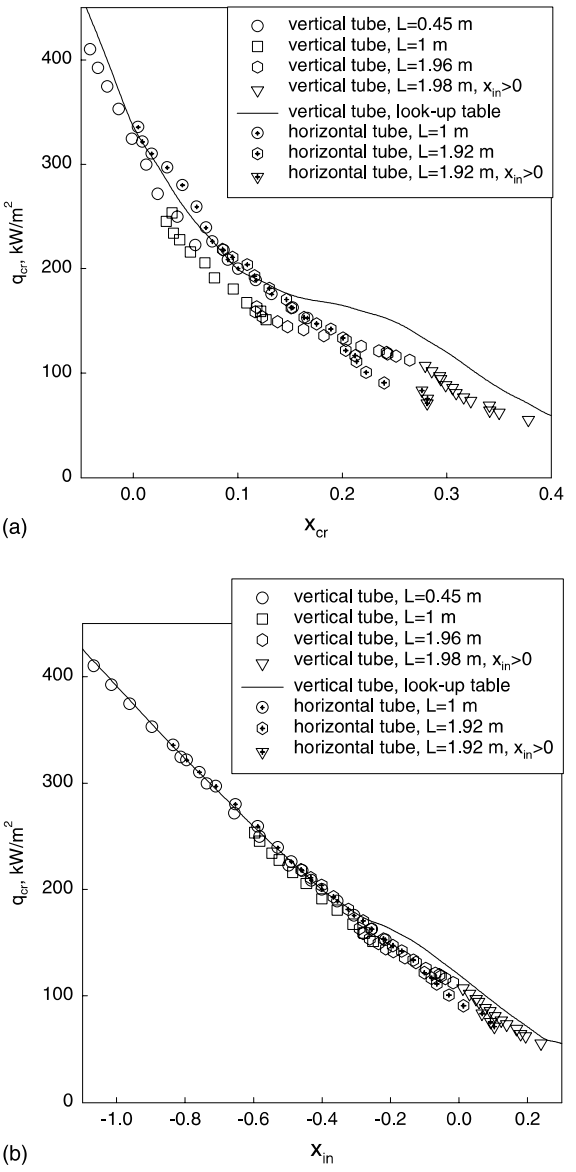

Fig. 4. Effect of quality on CHF in vertical and horizontal tubes ($D = 6.92$ mm): R-134a, $p = 1.31$ MPa, $G = 3000\ \mathrm{kg\,m^{-2}\,s^{-1}}$. (a) Effect of x_{cr}, (b) effect of x_{in}, data for tubes $L = 0.45$, 1, 1.92 and 1.96 m converted to $L = 1.98$ m; look-up table, $L = 1.98$ m.

No effect of the heated length is observed in Figs. 2b, 3b, 4b, 5b,d, 6b,d, 7b and d, thus demonstrating that the normalizing procedure described in Section 4.1 properly accounts for the heated length effect. The usual heated

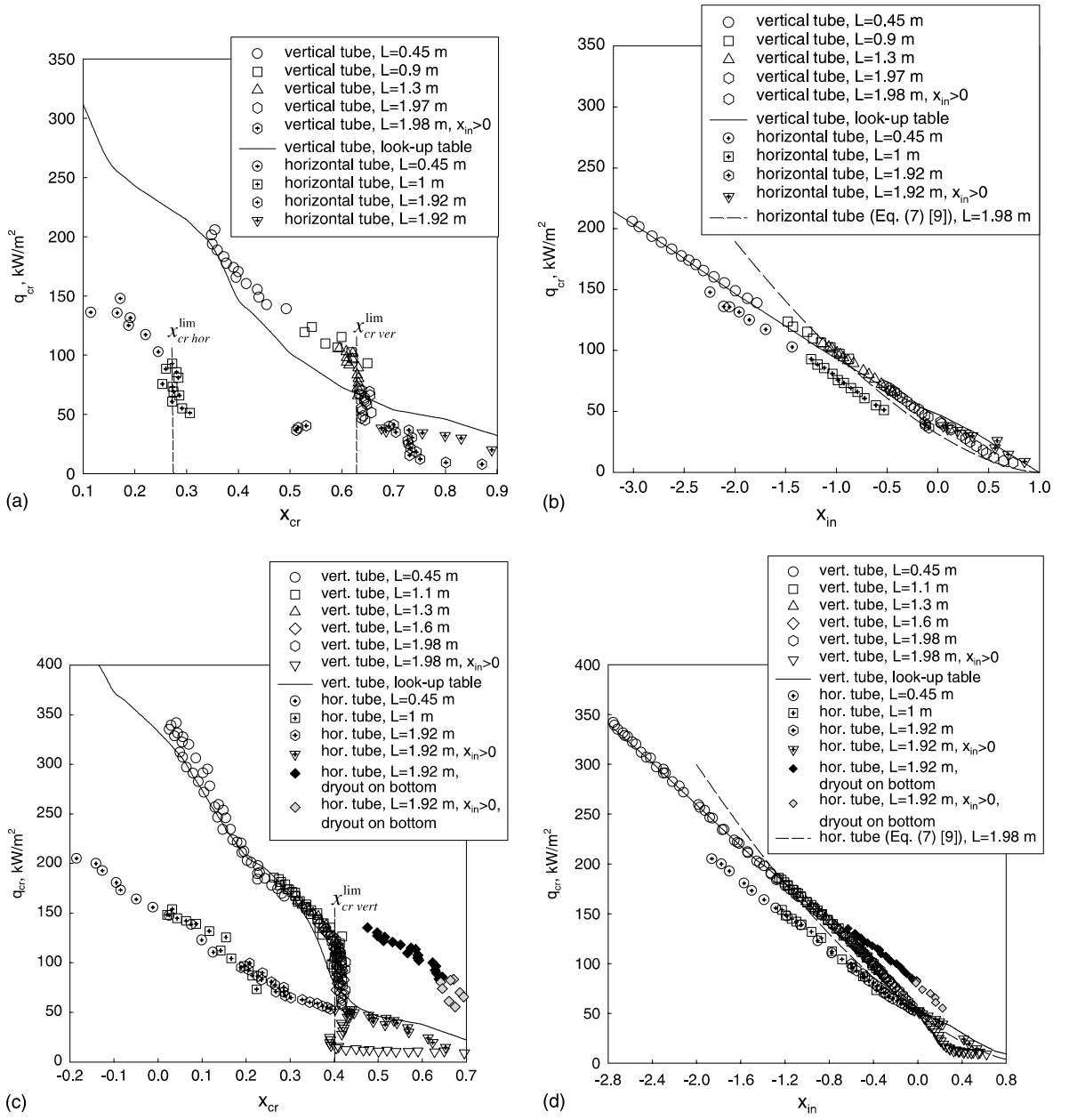

Fig. 5. Effect of quality on CHF in vertical and horizontal tubes ($D = 6.92$ mm): R-134a, $p = 1.67$ MPa. (a) Effect of x_{cr}, $G = 500$ kg m^{-2} s^{-1}, (b) effect of x_{in}, $G = 500$ kg m^{-2} s^{-1}; data for tubes $L = 0.45$, 0.9, 1, 1.3, 1.92 and 1.97 m converted to $L = 1.98$ m; look-up table, $L = 1.98$ m, (c) effect of x_{cr}, $G = 1000$ kg m^{-2} s^{-1}, (d) effect of x_{in}, $G = 1000$ kg m^{-2} s^{-1}; data for tubes $L = 0.45$, 1, 1.1, 1.3, 1.6 and 1.92 m converted to $L = 1.98$ m; look-up table, $L = 1.98$ m.

length effect is evident in Fig. 3c, where CHF versus x_{in} for various heated lengths is shown, and where x_{in} is not adjusted.

The agreement between the CHF look-up table [5] and the experimental values appears to be closer on a CHF versus x_{in} basis, rather than on a CHF versus x_{cr} basis, for the vertical tube CHF experimental data (as discussed by Pioro et al. [3]). Only at very low CHF values, for $x_{cr} > x_{cr}^{lim}$, does the look-up table value deviate from the measurements. Note that deviations from predictions should always be based on a constant x_{in}, since this quality is known prior to the CHF test. In

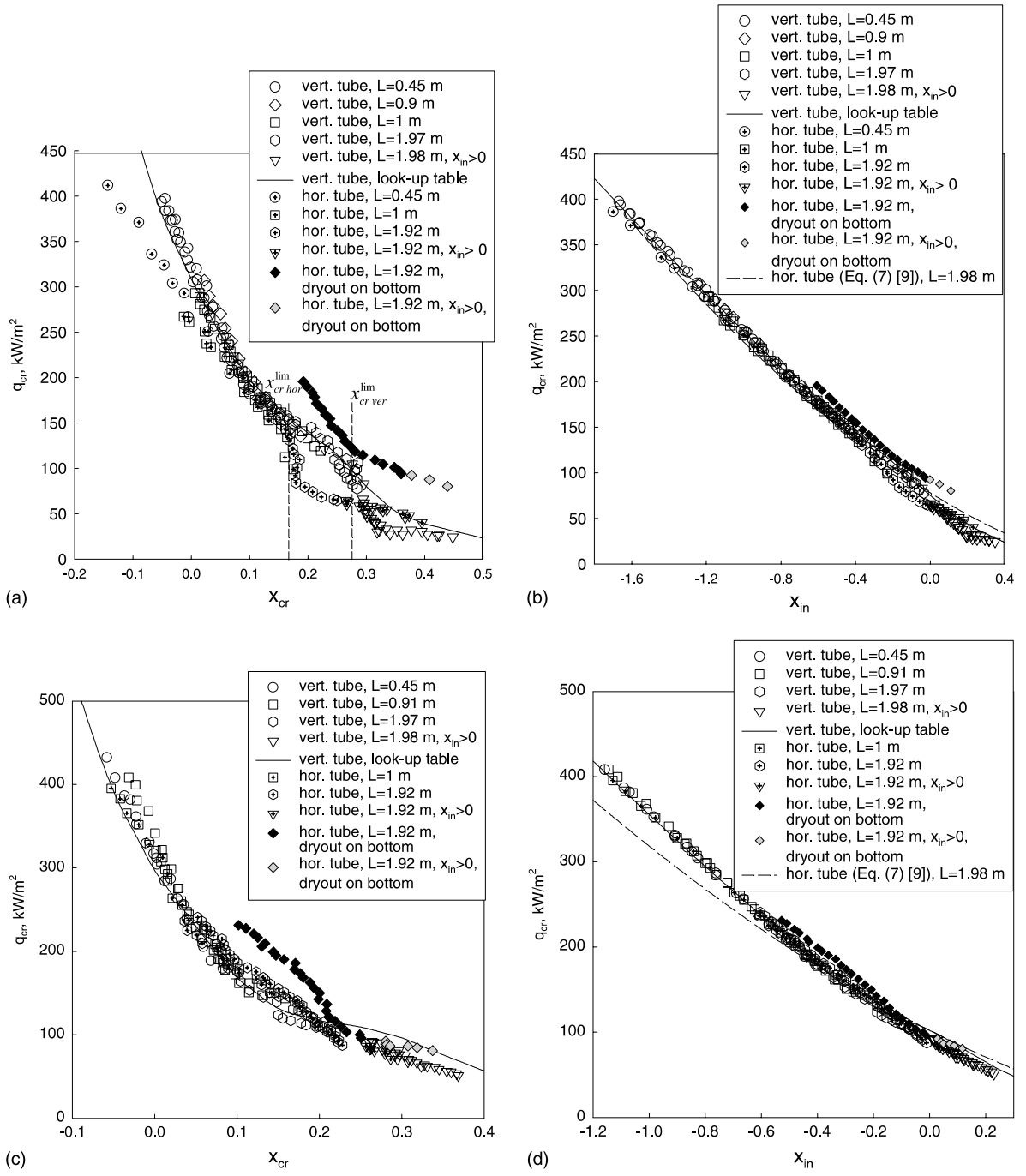

Fig. 6. Effect of quality on CHF in vertical and horizontal tubes ($D = 6.92$ mm): R-134a, $p = 1.67$ MPa. (a) Effect of x_{cr}, $G = 2000$ kg m^{-2} s^{-1}, (b) effect of x_{in}, $G = 2000$ kg m^{-2} s^{-1}, data for tubes $L = 0.45$, 0.9, 1, 1.92 and 1.97 m converted to heated length 1.98 m; look-up table, $L = 1.98$ m, (c) effect of x_{cr}, $G = 3000$ kg m^{-2} s^{-1}, (d) effect of x_{in}, $G = 3000$ kg m^{-2} s^{-1}, data for tubes $L = 0.45$, 0.91, 1, 1.92 and 1.97 m converted to heated length 1.98 m; look-up table, $L = 1.98$ m.

contrast, x_{cr} is not known prior to a CHF measurement; it is a function of CHF.

Figs. 3c, 5b,d, 6b and d show the CHF predictions for a horizontal orientation, calculated according to Merilo [9]. Eq. (7) does not match the experimental data very well.

Fig. 3c and d explain how small differences in CHF values in the inlet conditions approach can be exagger-

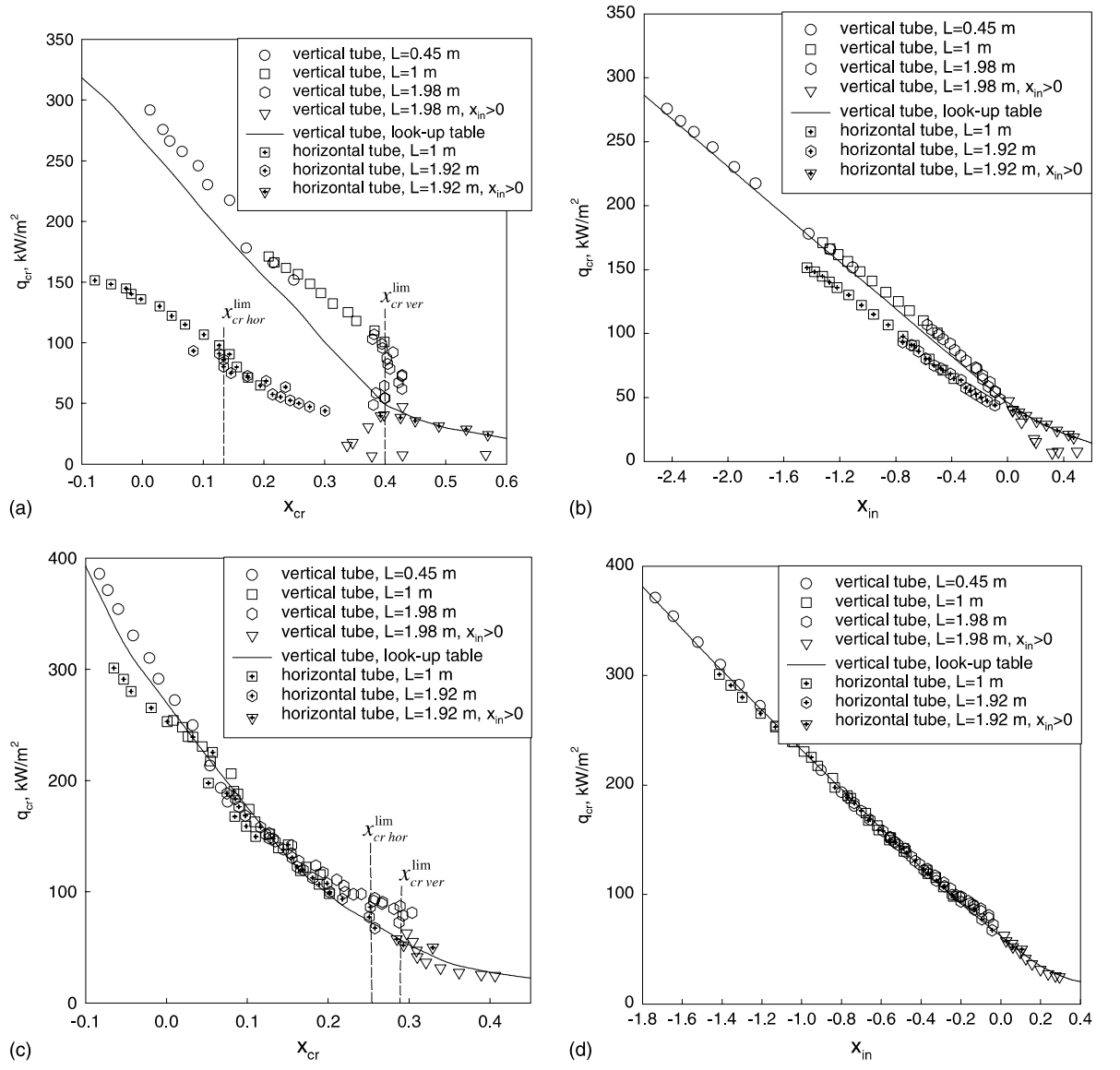

Fig. 7. Effect of quality on CHF in vertical and horizontal tubes ($D = 6.92$ mm): R-134a, $p = 2.03$ MPa. (a) Effect of x_{cr}, $G = 1000$ kg m^{-2} s^{-1}, (b) effect of x_{in}, $G = 1000$ kg m^{-2} s^{-1}, data for tubes $L = 0.45$, 1 and 1.92 m converted to heated length 1.98 m; look-up table, $L = 1.98$ m, (c) effect of x_{cr}, $G = 2000$ kg m^{-2} s^{-1}, (d) effect of x_{in}, $G = 2000$ kg m^{-2} s^{-1}, data for tubes $L = 0.45$, 1 and 1.92 m converted to heated length 1.98 m; look-up table, $L = 1.98$ m.

ated in the local conditions approach, within various ranges of critical qualities.

5. Discussion

5.1. Orientation effect

One of the primary contributions of this investigation is the observation that the orientation effect on CHF is closely linked to the type of CHF, which, in turn, is linked to the limiting critical quality. The modest reduction in CHF due to the horizontal orientation of the test section in Region I ($x_{cr} < x_{cr\,hor}^{lim}$) is reasonably well understood. Here, film dryout in vertical flow is entrainment-controlled and occurs simultaneously around the tube periphery. In horizontal flow, the liquid film on the top thins faster because of liquid film drainage to the bottom, and because of the reduced droplet deposition on the top part of the tube. The faster thinning of the

Table 2
Values of limiting critical quality and CHF drop (CF_{max}/CHF_{min}) in the limiting critical quality region for vertical and horizontal tubes ($D = 6.92$ mm)

p (MPa)	G (kg m^{-2} s^{-1})	Vertical tube			Horizontal tube		
		$x_{cr\,cal}^{lim}$ [25]	x_{cr}^{lim}	(CF_{max}/CHF_{min})	x_{cr}^{lim}	(CF_{max}/CHF_{min})	Δx_{cr}^{lim}
1.31	1000	0.48	0.48	2.5	0.18	1.8	0.30
1.31	2000	0.29	0.31	2.3	0.16	2.0	0.15
1.31	3000	0.21	–	–	0.20	1.3	–
1.67	500	0.67	0.63	10	0.27	3.2	0.36
1.67	1000	0.43	0.41	12	0.13	1.5	0.28
1.67	2000	0.25	0.29	3.3	0.15	2.1	0.14
2.03	1000	0.38	0.39	15	0.14	1.2	0.25

$\Delta x_{cr}^{lim} = \left(x_{cr}^{lim}\right)_{vert} - \left(x_{cr}^{lim}\right)_{hor}^{upper}$.

top film also leads to an earlier attainment of the "limiting critical quality" phenomenon, where the CHF drops rapidly. These findings are summarized in Table 2, where both the limiting critical qualities and the values of CHF_{max} (just before x_{cr}^{lim}) and CHF_{min} (just after x_{cr}^{lim}) are presented for the vertical and horizontal tests. The differences in x_{cr}^{lim} and the CHF ratios (CHF_{max}/CHF_{min}) decrease with increasing mass flux for a given pressure.

The significant reduction in CHF for Region II ($x_{cr\,hor}^{lim} < x_{cr} < x_{cr\,vert}^{lim}$) also appears to be somewhat obvious, a change in dryout type, from entrainment-controlled to deposition-controlled dryout has taken place on the top part of the horizontal tube; this has not yet occurred for the vertical flow case. In general, at the limiting critical quality, the fractional reduction in CHF for a horizontal tube is smaller than for a vertical tube (see Figs. 5a,c, 6a and 7a, and the data in Table 2).

The most surprising observation made in this study is that, in Region III ($x_{cr} > x_{cr\,vert}^{lim}$), the CHF can be higher for horizontal flow than for vertical flow (e.g., see Fig. 5a and c). This behavior may be explained by the enhanced deposition of droplets on the lower part of the tube (due to the action of the gravity force) resulting in a much thicker liquid film on the lower part of a horizontal tube, compared to the case of a vertical tube and the film spreading mechanism (creation of concentric waves on the liquid film surface). Thus, in the case of vertical flow, the CHF in Region III is prevented from occurring solely by droplet deposition. However, this is not the case in horizontal flow, for which the contribution of the thicker liquid film on the bottom provides a source of liquid to the top. This spreading of the liquid film to the top requires a higher vapor velocity and continuous interaction between vapor and slow-moving liquid film. This interaction can create large waves on the film surface at the lower part of the tube [35,36], which can result in the spreading of the liquid film to the upper part of a horizontal tube, thus suppressing CHF occurrence (so-called *concentric waves*). The results suggest that this mechanism of liquid transfer to the top can be more efficient then the deposition of liquid in Region III for vertical tubes.

5.2. Parametric trends

Heated length: In general, the effect of the heated length on CHF in vertical and horizontal orientations disappears on CHF versus x_{cr} graphs, or on plots of CHF versus x_{in} that are adjusted to a reference heated length, as described in Section 4.3. However, for short heated lengths ($L/D < 50$) in the vertical orientation, there is ample evidence from the literature that the CHF can be higher [5], especially for the annular flow region.

Orientation can affect the CHF in tubes of various heated lengths, especially if two-phase flow is present at the inlet of the test section and the two phases are well mixed. This orientation effect is due to the different time needed for the flow to stratify at the same two-phase flow conditions. In a longer tube, the time for stratification is longer than in a shorter tube, which leads to a lower CHF value. Horizontal tubes with short heated lengths tend to have similar CHF values, compared to those in vertical tubes.

Pressure: The effect of pressure ($p = 1.31$–2.03 MPa) on CHF is shown in Fig. 8a and b for two mass flux values (1000 and 2000 kg m^{-2} s^{-1}). Both flow orientations show that, in general, a lower pressure results in a higher CHF (this universal trend is observed in all fluids for p/p_{cr} ratios greater than about 0.2). The orientation effect on CHF appears to be less strong at higher pressures and at $G = 2000$ kg m^{-2} s^{-1} (e.g., compare Figs. 4a, 6a and 7c). One possible reason for this behavior is that, here, the density difference is smaller and hence, the tendency towards stratification is correspondingly less strong. This could also explain the smaller value for $x_{cr\,hor}^{lim} - x_{cr\,vert}^{lim}$ at higher pressures. Note that this is partially offset by the lower velocity at higher pressures, which is responsible for the weaker momentum forces at high pressures [14].

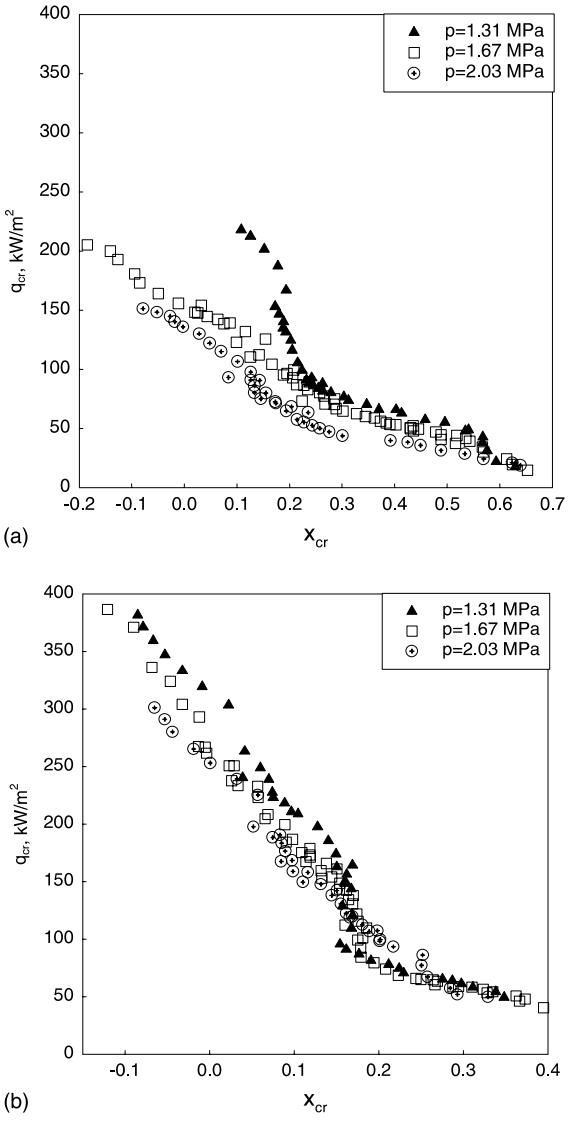

Fig. 8. Effect of critical quality on CHF in horizontal tube at different pressures: R-134a, $D = 6.92$ mm, $L = 0.45$–1.92 m. (a) $G = 1000\ \mathrm{kg\,m^{-2}\,s^{-1}}$, (b) $G = 2000\ \mathrm{kg\,m^{-2}\,s^{-1}}$.

Mass flux: The effect of mass flux on CHF is shown in Fig. 9a–c at three pressure values (1.31, 1.67 and 2.03 MPa). The opposite trends of mass flux on CHF for vertical [3] and horizontal flow, especially in the annular flow region at $x_{cr} < x_{cr}^{lim}$ are due to two different mechanisms:

(i) For vertical flow, film depletion by entrainment is strongest at the higher mass fluxes; hence, the inverse CHF/mass flux trend occurs at higher qualities.
(ii) For horizontal flow, the orientation effect becomes significant for mass fluxes less than 2000 $\mathrm{kg\,m^{-2}\,s^{-1}}$, and this counteracts the film depletion effect. This removes the inverse CHF / mass flux trend and results in either a small mass flux effect or a decrease in CHF with a decrease in mass flux (see Fig. 9b, $G = 500\ \mathrm{kg\,m^{-2}\,s^{-1}}$).

5.3. Effect of fluid type

Although R-134a was used as the coolant in this experiment, it is useful to discuss the impact of the orientation effect in other fluids, as R-134a CHF results are frequently converted into water-equivalent values using the fluid-to-fluid modeling relationships (Eqs. (1)–(5) given in Section 1). The orientation effect on CHF is significantly stronger in R-134a than in water at equivalent conditions, for the following reasons: (i) the density difference at equivalent pressures is about 40% greater, and (ii) the equivalent mass flux is about 30% lower. The net result is that the momentum forces, which counteract the tendency towards stratification, are about 65% smaller in water than in R-134a. This can also be seen by the modified Froude number of Celata and Mariani [21] (Eq. (12)) for equivalent conditions; the Froude number in R-134a is about 50% smaller than that for water.

The differences in the Froude numbers and other fluid properties between R-134a and water also result in different limiting critical qualities. Hence, Regions I–III will cover different ranges of quality. The quality range of Region II, where the orientation effect was found to be the most pronounced, can be expressed by $\Delta x_{cr}^{lim} = x_{cr\,vert}^{lim} - x_{cr\,hor}^{lim}$. This value is much smaller (at equivalent conditions) for water [30] than for R-134a (see Table 2). Note that Δx_{cr}^{lim} decreases with increasing flow, although the effect of pressure on Δx_{cr}^{lim} is less clear.

6. Conclusions and final remarks

1. CHF experiments were performed in horizontal and vertical circular tubes in R-134a covering several pressures and mass fluxes. To provide as wide a range of critical qualities as possible, various heated lengths and two-phase flow at the test-section inlets were used.
2. At low-to-medium flows, CHF values for a horizontal tube cooled with R-134a can be significantly lower than those for a vertical tube. The largest decrease in horizontal tube CHF, in comparison with that in a vertical tube, was observed at the lowest flow and for the region where $x_{cr\,hor}^{lim} < x_{cr} < x_{cr\,vert}^{lim}$.
3. The most surprising observation was that, for critical qualities higher than the limiting critical quality for vertical flow, the CHF values for horizontal tubes can be higher than those for vertical tubes. This

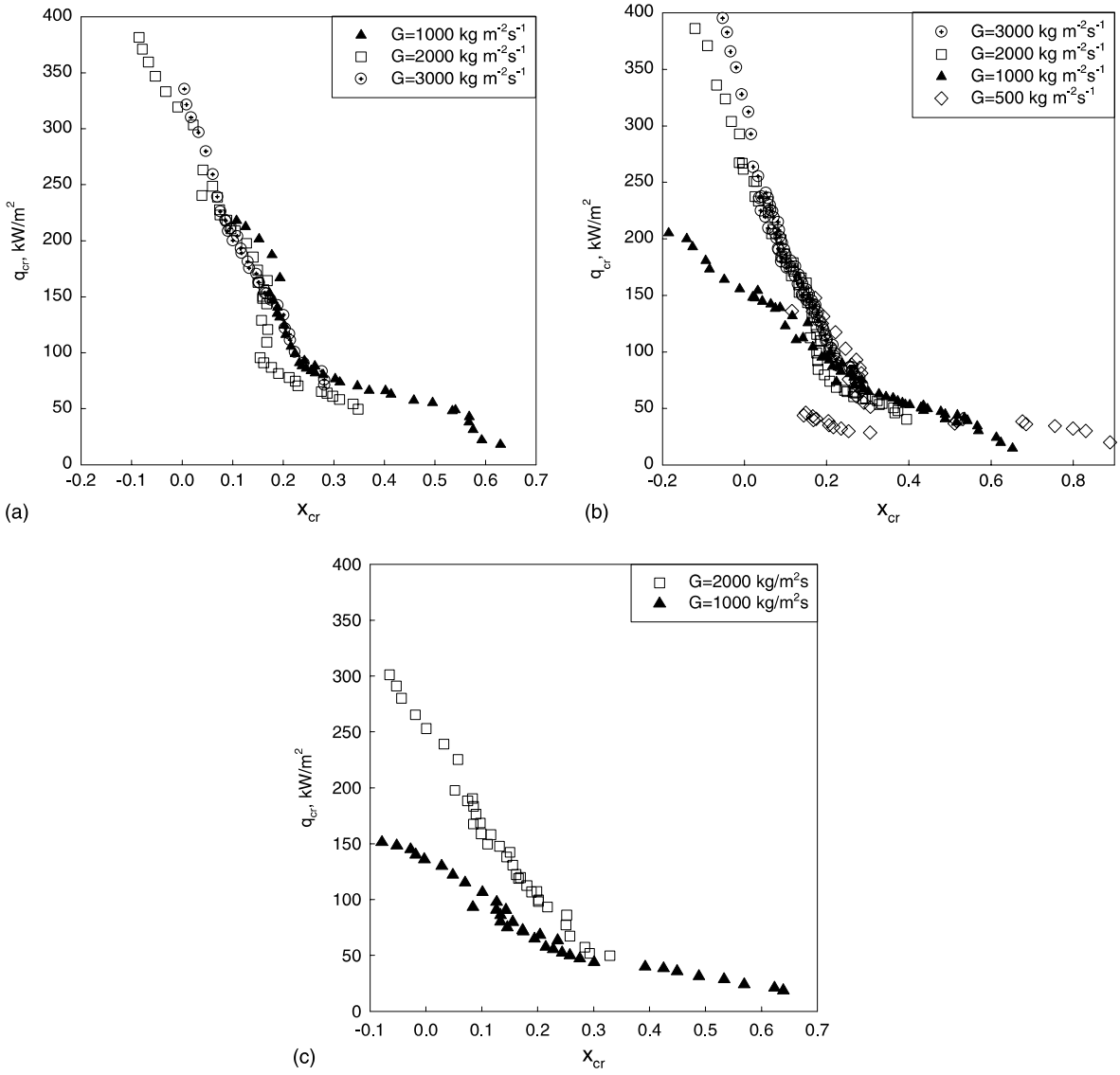

Fig. 9. Effect of critical quality on CHF in horizontal tube at different mass fluxes: R-134a, $D = 6.92$ mm, $L = 0.45$–1.92 m. (a) $p = 1.31$ MPa, (b) $p = 1.67$ MPa, (c) $p = 2.03$ MPa.

behavior is thought to be due to the enhanced deposition of droplets on the lower part of the horizontal tube (because of the action of the gravity force) resulting in a much thicker liquid film on the lower part of a horizontal tube, compared to the case of a vertical tube and the film spreading mechanism (creation of concentric waves on the liquid film surface).

4. Usually, initial dryout in a horizontal tube was observed to occur at the downstream end. Under some flow conditions, initial dryout can occur at locations that are well upstream from the downstream end of a horizontal tube.
5. The CHF fluid-to-fluid modeling technique developed for vertical flow does not apply for horizontal flow at conditions where stratification effects become significant, i.e., at mass fluxes less than 3500 $\mathrm{kg\,m^{-2}\,s^{-1}}$. At high mass fluxes, the effect of orientation on CHF was not significant.

Acknowledgements

The financial support provided by AECL and NSERC is gratefully acknowledged.

References

[1] R.M. Tain, S.C. Cheng, D.C. Groeneveld, Critical heat flux measurements in a round tube for CFC's and CFC alternatives, Int. J. Heat Mass Transfer 36 (1993) 2039–2049.

[2] D.C. Groeneveld, D. Blumenrohr, S.C. Cheng, et al., Laboratories using different modeling fluids, in: Proceedings of the 4th International Topical Meeting on Nuclear Thermal Hydraulics (NURETH-4), Salt Lake City, Utah, USA, vol. II. 1992, pp. 531–538.

[3] I.L. Pioro, D.C. Groeneveld, S.C. Cheng, et al., Comparison of CHF measurements in R-134a cooled tubes and the water CHF look-up table, Int. J. Heat Mass Transfer 44 (1) (2001) 73–88.

[4] D.C. Groeneveld, S. Doerffer, R.M. Tain, et al., Fluid-to-fluid modeling of the critical heat flux and post dryout heat transfer, in: Proceedings of the World Congress on Experimental Heat Transfer, Fluid Mechanics and Thermodynamics, Brussels, Belgium, vol. 2, 1997, pp. 859–867.

[5] D.C. Groeneveld, L.K.H. Leung, P.L. Kirillov, et al., The 1995 look-up table for critical heat flux in tubes, Nucl. Eng. Design 163 (1996) 1–23.

[6] K.M. Becker, Measurement of burnout conditions for flow of boiling water in horizontal round tubes, in: Report AERL–1262, Aktiebolaget Atomenergi, Sweden, 1971, pp. 1–25.

[7] J.M. Robertson, Dryout in horizontal hairpin waste-heat boiler tubes, Symp. Ser. AIChE J. 69 (131) (1973) 55–72.

[8] M. Merilo, Critical heat flux experiments in a vertical and horizontal tube with both Freon-12 and water as coolant, Nucl. Eng. Design 44 (1977) 1–16.

[9] M. Merilo, Fluid-to-fluid modeling and correlation of flow boiling crisis in horizontal tubes, Int. J. Multiphase Flow (5) (1979) 313–325.

[10] M. Merilo, S.Y. Ahmad, The effect of diameter on vertical and horizontal flow boiling crisis in a tube cooled by Freon-12, Report AECL–6485, AECL, Chalk River Nuclear Laboratories, Chalk River, Ontario, Canada, March 1979, pp. 1–51.

[11] W. Köhler, D. Hein, Influence of the wetting state of a heated surface on heat transfer and pressure loss in an evaporator tube, in: International Agreement Report NUREG/IA–0003, 1986, pp. 63–79.

[12] Y. Taitel, A.E. Dukler, A model for predicting flow regime transitions in horizontal and near horizontal gas–liquid flow, AIChE J. 22 (1976) 47–55.

[13] D.C. Groeneveld, S.C. Cheng, T. Doan, AECL-UO critical heat flux look-up table, Heat Transfer Eng. 7 (1986) 46–62.

[14] Y.L. Wong, D.C. Groeneveld, S.C. Cheng, CHF prediction for horizontal tubes, Int. J. Multiphase Flow 16 (1990) 123–138.

[15] Y. Taitel, A.E. Dukler, Flow pattern transition in gas–liquid systems measurement and modelling, in: G.F. Hewitt, J.M. Delhaye, N. Zuber (Eds.), Multiphase Science and Technology, vol. 2, Hemisphere Publishing Corporation, Washington, DC, USA, 1986, pp. 1–94.

[16] Y.L. Wong, Generalized CHF prediction for horizontal tubes with uniform heat flux, Thesis of Master of Applied Science, Mechanical Engineering Department, University of Ottawa, Ottawa, Ontario, Canada, June, 1988.

[17] P. Saha, N. Zuber, Point of net vapor generation and vapor void fraction in subcooled boiling, in: Proceedings of the 5th International Heat Transfer Conference, Tokyo, Japan, vol. 4, 1974, pp. 175–179.

[18] L.S. Tong, Y.S. Tang, Boiling Heat Transfer and Two-Phase Flow, second ed., Taylor & Francis, Bristol, PA, 1997, pp. 140–147, 387–391.

[19] Boiling Inside Tubes: Critical Heat Flux for Flow in Uniformly Heated Horizontal Tubes, Engineering Sciences Data Unit (ESDU), Item #88001, November, 1989.

[20] V. Kefer, W. Köhler, W. Kastner, Critical heat flux (CHF) and post-CHF heat transfer in horizontal and inclined evaporator tubes, Int. J. Multiphase Flow 15 (3) (1989) 385–392.

[21] G.P. Celata, A. Mariani, CHF and post-CHF (post-dryout) heat transfer, Chapter 17, in: S.G. Kandlikar, M. Shoji, V.K. Dhir (Eds.), Handbook of Phase Change. Boiling and Condensation, Taylor & Francis, Philadelphia, PA, 1999, pp. 450–451, 464–465.

[22] G.P. Celata, M. Cumo, A. Mariani, Enhancement of CHF water subcooled flow boiling in tubes using helically coiled wires, Int. J. Heat Mass Transfer 37 (1) (1993) 53–67.

[23] G.F. Hewitt, Critical heat flux in flow boiling, Proceedings of the 6th International Heat Transfer Conference, Toronto, Canada, vol. 6, 1978, pp. 143–171.

[24] J.B. Kitto Jr., Critical heat flux and the limiting quality phenomenon, AIChE J. Symp. Ser. Heat Transfer 76 (199) (1980) 57–78.

[25] I.L. Pioro, S.C. Cheng, A. Vasić, R. Felisari, Some problems for bundle CHF prediction based on CHF measurements in simple flow geometries, Nucl. Eng. Design 201 (2/3) (2000) 189–207.

[26] I.L. Pioro, D.C. Groeneveld, S.C. Cheng, et al., Effect of flow obstruction shape on the critical heat flux, in: Proceedings of 8th International Conference on Nuclear Engineering (ICONE-8), Baltimore, Maryland, USA, 2–6 April 2000, Paper 8350 (Track 7.04), pp. 1–15.

[27] I.L. Pioro, S.C. Cheng, A. Vasić, I. Salah, Experimental evaluation of the limiting critical quality values in circular and non-circular flow geometries, Nucl. Eng. Design 190 (1999) 317–339.

[28] I.L. Pioro, S.C. Cheng, A. Vasić, S. Doerffer, Investigation of the effect of non-circular geometry on the critical heat flux under saturated flow boiling conditions, Recent Research Developments in Heat, Mass & Momentum Transfer, vol. 2, Research Signpost Publisher, India, 1999, pp. 21–39.

[29] I.L. Pioro, S.C. Cheng, D.C. Groeneveld, et al., Effect of flow obstructions in a circular tube on the critical heat flux (CHF), in: Proceedings of the 17th Canadian Congress of Applied Mechanics (CANCAM 99), Hamilton, Ontario, Canada, 30 May–June 3, 1999, pp. 267–268.

[30] A.M. Kutepov, L.S. Sterman, N.G. Styushin, Hydrodynamics and Heat Transfer During Vaporization, Vysshaya Shkola, Moscow, 1977, pp. 230–231.

[31] I.L. Pioro, S.S. Doerffer, S.C. Cheng, Experimental investigation of the limiting critical quality in horizontal tubes cooled with water and R-134a, in: Proceedings of 10th International Conference on Nuclear Engineering (ICONE-10), Arlington, Virginia, DC, USA, April 14–18, 2002, Paper (Track 7.04), pp. 1–15.

[32] L.S. Pioro, I.L. Pioro, Industrial Two-Phase Thermosyphons, Begell House Inc., New York, NY, USA, 1997, pp. 1–288.
[33] I.L. Pioro, Y. Lee, New correlations for critical heat flux of two-phase closed and open loop thermosyphons which account for conjugation, in: Proceedings of the 9th International Heat Pipe Conference, Albuquerque, NM, USA, 1–5 May 1995, Advances in Heat Pipe Science and Technology, vol. 1. 1997, pp. 514–519.
[34] Y. Lee, I.L. Pioro, Ch.-S. Yim, Effect of conjugation on critical heat flux of two-phase closed thermosyphons, in: Proceedings of the 10th International Heat Transfer Conference, Brighton, UK, vol. 6. 14–18 August 1994, pp. 217–221.
[35] T. Fukano, A. Ousaka, Prediction of the circumferential distribution of film thickness in horizontal and near-horizontal gas–liquid annular flows, Int. J. Multiphase Flow 15 (3) (1989) 403–419.
[36] A.G. Flores, K.E. Crowe, P. Griffith, Gas-phase secondary flow in horizontal, stratified and annular two-phase flow, Int. J. Multiphase Flow 21 (2) (1995) 207–221.